

# A Parametric Study of the Behavior of the Angular Momentum Vector During Spin Rate Changes of Rigid-Body Spacecraft

James M. Longuski\* and Tooraj Kia†

*Jet Propulsion Laboratory, California Institute of Technology, Pasadena, California*

During a spinup or spindown maneuver of a spinning spacecraft, it is usual to have not only a constant body-fixed torque about the desired spin axis, but also small undesired constant torques about the transverse axes. The undesired torques cause the orientation of the angular momentum vector to change in inertial space. Since an accurate approximate analytic solution is available for the angular momentum vector as a function of time, this behavior can be studied for large variations of dynamic parameters such as the initial spin rate, the inertial properties, and the torques. As an example, the spinup and spindown maneuvers of the Galileo spacecraft were studied, and as a result very simple heuristic solutions were discovered which provide very good approximations to the parametric behavior of the angular momentum vector orientation.

## Nomenclature

$f(x)$	= probability density function
$H$	= angular momentum vector
$I_i$	= moment of inertia about the $i$ -axis
$t_f$	= spin-change duration
$\Delta x$	= variations about $x$
$\epsilon_x$	= percent $x$ -variable error
$\xi$	= nutation angle
$\rho$	= radial distance from the center of spiral
$\rho_0$	= distance from origin to the center of spiral
$\sigma_x$	= $x$ -variable error variance
$\phi_i$	= Eulerian angles
$\omega_i$	= $i$ -axis angular rotation rate
$\omega_{i0}$	= $i$ -axis rotation rate at $t=0$

## Introduction

THE study of the parametric behavior of the angular momentum vector during spinup and spindown maneuvers of rigid-body spacecraft is greatly facilitated by an analytic solution,  $H(t)$ . While it is a simple matter to obtain the solution numerically by integrating the equations of motion on a computer, it is not so easy to find out how the final conditions vary as each of the dynamic parameters involved is perturbed. This is because a separate simulation is required for each perturbation. Such simulation can be expensive and time consuming. In this study, a computational algorithm was written based on the analytic solutions<sup>1</sup> for Euler's equations of motion, the Eulerian angles, and the angular momentum vector, so that the final angular momentum vector could be found quickly and efficiently without numerical integration.

The primary interest is focused on the variation of  $H(t_f, \omega_{x0}, \omega_{y0}, \omega_{z0}, M_x, M_y, M_z, I_x, I_y, I_z)$  as each of the 10 parameters indicated is varied separately from its nominal value. Thus, plots are displayed which show the functional behavior of  $H_f$  in terms of  $\Delta\omega_{x0}$ , in terms of  $\Delta\omega_{y0}$ , etc. Specific numerical parameters from the Galileo spacecraft spinup and spindown maneuvers were used as an example.

The perturbations corresponded mainly to the  $3\sigma$  (standard deviations) values or larger. Using a deterministic performance analysis approach, an estimate of the  $H$  vector variations from its nominal final orientation is found. Since some of the perturbations, such as  $M_x$  and  $M_y$ , produced a linear variation of  $H_f$ , these were examined for much greater ranges than the  $3\sigma$  values. This approach revealed simple heuristic relations for the error model. Finally, the results of Monte Carlo simulation are compared to the heuristic estimates and conclusions are drawn for this particular and similar examples.

## Solution of Euler's Equations of Motion

Euler's equations of motion of a rigid body are

$$\begin{aligned} M_x &= I_x \dot{\omega}_x + (I_z - I_y) \omega_y \omega_z \\ M_y &= I_y \dot{\omega}_y + (I_x - I_z) \omega_z \omega_x \\ M_z &= I_z \dot{\omega}_z + (I_y - I_x) \omega_x \omega_y \end{aligned} \quad (1)$$

An accurate approximate analytic solution to Eqs. (1) is obtained for near-symmetric rigid bodies subject to arbitrary constant moments by assuming

$$\omega_z = M_z t / I_z + \omega_{z0} \quad (2)$$

When  $I_x = I_y$ , then Eq. (2) is exact as in the Bødewadt<sup>2</sup> solution, but when  $I_x \approx I_y$ , the approximation provides very useful accurate solutions, particularly when  $\omega_x$  and  $\omega_y$  are small, which is usually the case for spin-stabilized spacecraft. The solutions for  $\omega_x$  and  $\omega_y$  are given in Ref. 1.

## Approximate Solution for the Eulerian Angles

The kinematic equations of motion for a type 1: 3-1-2 Euler angle rotation are<sup>3</sup>

$$\begin{aligned} \dot{\phi}_x &= \omega_x \cos \phi_y + \omega_z \sin \phi_y \\ \dot{\phi}_y &= \omega_y - (\omega_z \cos \phi_y - \omega_x \sin \phi_y) \tan \phi_x \\ \dot{\phi}_z &= (\omega_z \cos \phi_y - \omega_x \sin \phi_y) \sec \phi_x \end{aligned} \quad (3)$$

For the case of symmetric rigid bodies subject to constant moments, Bødewadt<sup>2</sup> proposed a solution of Eqs. (3) (and all other versions of Euler angle rotations) which has been shown

Presented as Paper 82-1467 at the AIAA/AAS Astrodynamics Conference, San Diego, Calif., Aug. 9-11, 1982; received Sept. 13, 1982; revision received June 7, 1983. Copyright © American Institute of Aeronautics and Astronautics, Inc., 1982. All rights reserved.

\*Senior Engineer, Guidance and Control Section.

†Member of Technical Staff, Guidance and Control Section.

to be valid only for a very restricted set of conditions and incorrect in general.<sup>4</sup>

A highly accurate approximate analytic solution for the Eulerian angles for a near-symmetric rigid body has been found corresponding to case 3 of Bödewadt. The main restrictions on the solution are that two of the Eulerian angles must remain small and the parameter  $|\omega_z|/\sqrt{(|\dot{\omega}_z|)}$  must remain large.

### Solution for the Angular Momentum Vector

With the analytic results for the angular velocities,  $\omega_x$ ,  $\omega_y$ , and  $\omega_z$ , and the type 1:3-1-2 Euler angles,  $\phi_x$ ,  $\phi_y$ , and  $\phi_z$ , the approximate analytic solution for the angular momentum vector in inertial space can be constructed easily:

$$\begin{Bmatrix} H_x \\ H_y \\ H_z \end{Bmatrix} = A \begin{Bmatrix} I_x \omega_x \\ I_y \omega_y \\ I_z \omega_z \end{Bmatrix} \quad (4)$$

where  $A$  is the transformation matrix based on the Eulerian angles.

### An Example of Parametric Behavior of the Angular Momentum Vector

In this section we will study the parametric behavior of the angular momentum vector during spinup and spindown maneuvers for a specific spacecraft—the Galileo. The purpose here is to obtain practical results which may be used in probabilistic error models. It will be demonstrated that simple heuristic solutions can be used to express the orientation of the final angular momentum vector and that perturbation of these solutions provide the secular effects. In addition it is shown that the periodic effects can be closely modeled by a ring distribution. The final result is a probabilistic error model which can be used to assess dispersions of the angular momentum vector during spinup and spindown maneuvers. The result is confirmed by the classical Monte Carlo analysis.

Galileo is a dual-spin, dual-purpose spacecraft. Scheduled for a 1986 launch toward Jupiter, it will release a probe into the Jovian atmosphere and then orbit the planet for about 20 months gathering and transmitting scientific data. The spacecraft is usually in dual-spin mode, but during  $\Delta V$  maneuvers the mode is changed to single-spin by locking the rotor and stator together. It is then spun up to 1 rad/s, from a nominal of 0.306 rad/s, prior to an axial  $\Delta V$  burn. This increases the stability margin and the accuracy of the maneuver. After the burn, the spacecraft is spun down to 0.306 rad/s. The thruster configuration is illustrated in Fig. 1 where S2A and -S1A are the primary spinup and spindown thrusters, respectively, and S2B and -S1B are backups.

The nominal  $H$  pointing during the spinup maneuver is shown in Fig. 2, which was generated from Eq. (4). Since the angles involved are very small, the quantities  $H_x/H_z$  and  $H_y/H_z$  are used to describe the orientation of the angular momentum vector in inertial space. The analytic solutions were tested by employing the Advanced Continuous Simulation Language (ACSL) to perform a very precise numerical integration by the Runge-Kutta method. It was found that the analytic solution for the  $H$  pointing produced errors no greater than an order of  $10^{-5}$  rad throughout the maneuver duration.

It is very interesting to note that the radial distance of the spiral path exhibited in Fig. 2 from its center can be approximated accurately, in this particular case, by the heuristic relation

$$\rho(t) = (M_x^2 + M_y^2)^{1/2} / I_z \omega_z^2 \quad (5)$$

where

$$\omega_z \approx M_z t / I_z + \omega_{z0}$$

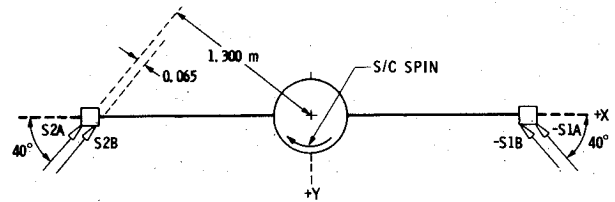


Fig. 1 Spin thruster configuration.

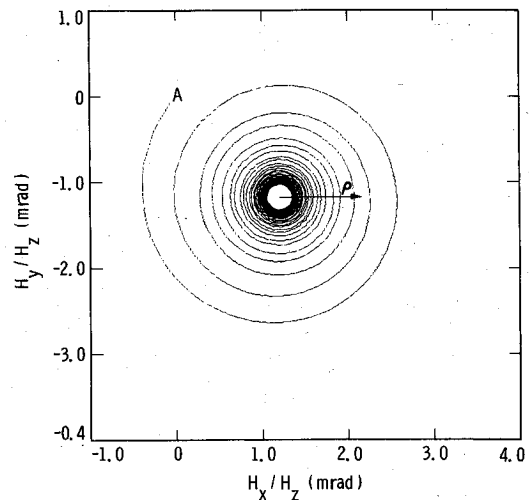


Fig. 2 Nominal orientation of the angular momentum vector in inertial space during spinup maneuver.

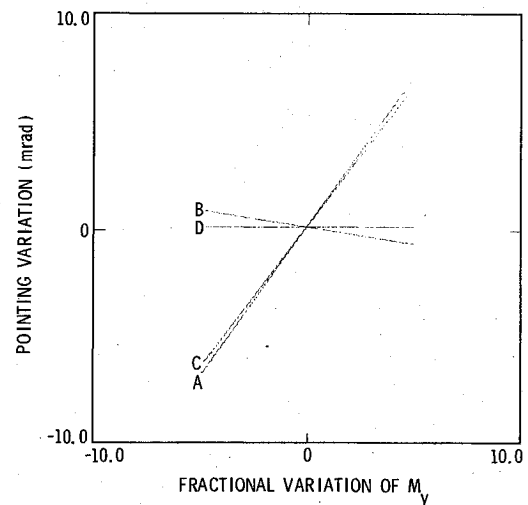


Fig. 3 Variational orientation of  $H_f$  during spinup for  $M_y \pm 500\%$ . a) x axis, b) y axis, c) x axis heuristic, and d) y axis heuristic.

The center point of the spiral is also approximated by the simple heuristic relations:

$$x = -M_y / I_z \omega_{z0}^2, \quad y = M_x / I_z \omega_{z0}^2 \quad (6)$$

These solutions were inspired from the case of  $M_z = 0$ , in which they can be derived for small angles  $\phi$  and  $\phi_y$ . In this situation of constant spin rate, the angular momentum vector precesses about the direction given by  $x$  and  $y$ , in a closed curve.

Now the parametric behavior of the final angular momentum vector orientation will be examined. For the purpose of this study it was assumed that the correct final spin rate is always achieved. This can be accomplished by using

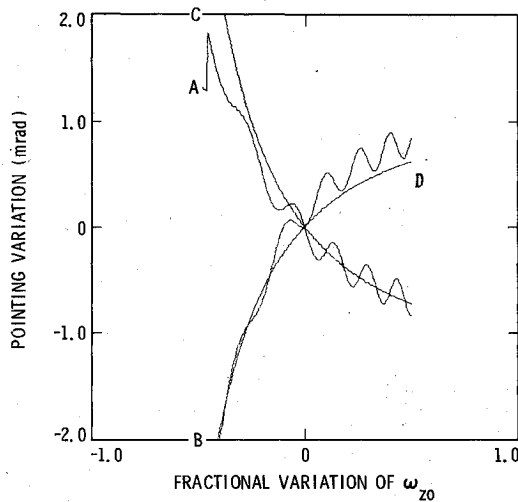


Fig. 4 Variational orientation of  $H_f$  during spinup for  $\omega_{z0} \pm 50\%$ . a) x axis, b) y axis, c) x axis heuristic, and d) y axis heuristic.

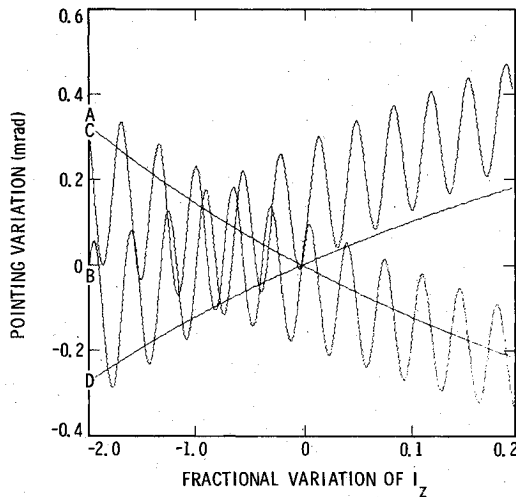


Fig. 5 Variational orientation of  $H_f$  during spinup for  $I_z \pm 20\%$ . a) x axis, b) y axis, c) x axis heuristic, and d) y axis heuristic.

appropriate sensors such as star trackers or sun sensors in a feedback control system. An alternative approach was also studied involving a controlled burn time which is open loop, but these results are not presented here.

Let  $H_f$  represent the nominal angular momentum at the end of the spin rate change maneuver and let  $H_f(\Delta\alpha)$  represent the vector when parameter  $\alpha$  is perturbed by  $\Delta\alpha$ . Using ACSL Galileo spin-change dynamics were simulated. The simulation was based on the analytic solutions derived from Eqs. (1-4). The method of deterministic performance analysis was employed to calculate and plot the variational behavior of the angular momentum vector  $H_f(\Delta\alpha) - H_f$  as  $\Delta\alpha$  is varied from extreme negative to extreme positive values. A few sample cases for spinup and spindown modes are shown in Figs. 3-13.

These results indicate that parametric behavior can be described as either periodic, secular, or a combination of periodic and secular effects. Perturbation of the transverse torques resulted in a secular perturbation of the final angular momentum vector, while perturbation of  $I_z$ ,  $M_z$ , and  $\omega_z$  produced combined periodic and secular variations with periodic effects being the dominant factor, except for  $\omega_z$  in the spinup mode. Perturbations of  $I_x$  and  $I_y$  resulted in very small variations. Small changes in the initial values of the transverse angular velocities produced a linear (or secular) effect on the final angular momentum vector.

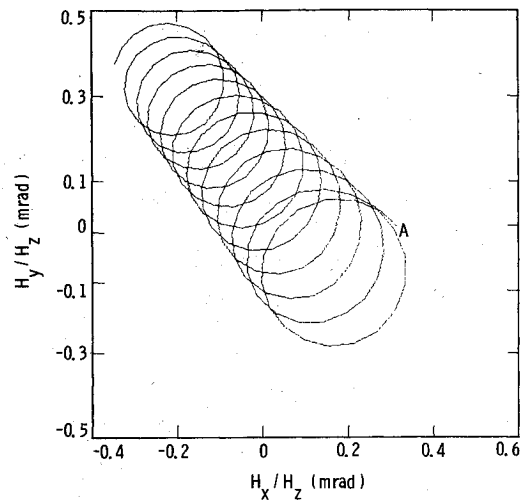


Fig. 6 Variational orientation of  $H_f$  during spinup for  $I_z \pm 20\%$ .

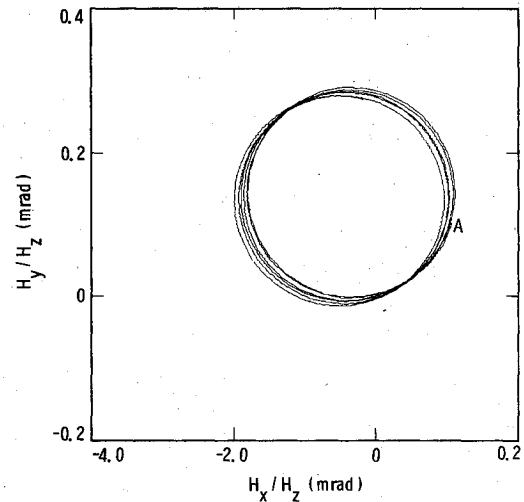


Fig. 7 Variational orientation of  $H_f$  during spinup for  $M_z \pm 50\%$ .

Figures 3-5 have the heuristic solutions, as given by Eqs. (6), superimposed on the plots. For zero initial transverse velocities the heuristic solution provides a good approximation of the secular and average periodic effects. The effect of nonzero initial transverse angular velocities is to produce an initial nutation angle  $\xi$ , which is defined as the angle between the  $z$ -axis and the angular momentum vector. The initial nutation angle is given by

$$\tan \xi = (I_x^2 \omega_{x0}^2 + I_y^2 \omega_{y0}^2)^{1/2} / I_z \omega_{z0} \quad (7)$$

Normally the transverse velocities are nearly zero and there is no nutation angle. Perturbations of  $\omega_{x0}$  and  $\omega_{y0}$  result in a linear perturbation of  $H_f$ . This is shown in Fig. 7 for variations in  $\omega_{x0}$ .

Since Eq. (5) provides a good estimate for the average pointing error, it also may be used to estimate the variance due to the secular terms. Let  $\epsilon_x = dx/x$  signify the error in  $x$ , then,

$$\epsilon_{\rho 0} = \frac{d\rho_0}{\rho_0} = \frac{dM}{M} - \frac{dI_z}{I_z} - \frac{2d\omega_z}{\omega_z} \quad (8)$$

where

$$M = (M_x^2 + M_y^2)^{1/2}$$

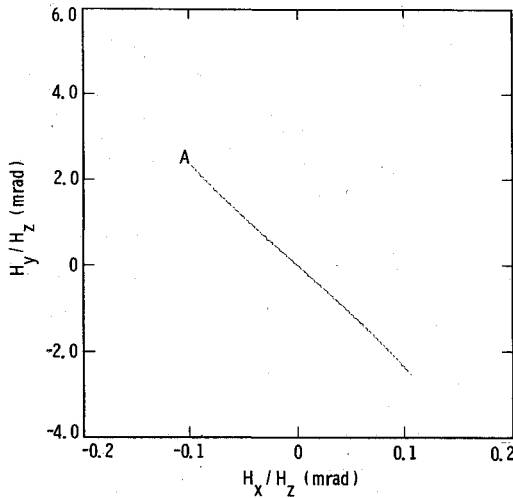


Fig. 8 Variational orientation of  $H_f$  during spinup for  $\omega_{x0} \pm 0.0005$  rad/s.

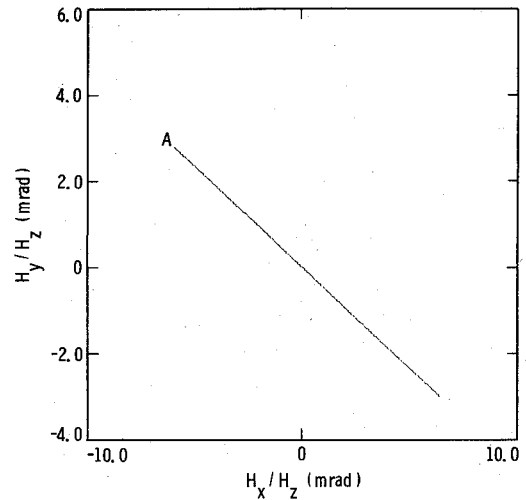


Fig. 10 Variational orientation of  $H_f$  during spindown for  $M_y \pm 500\%$ .

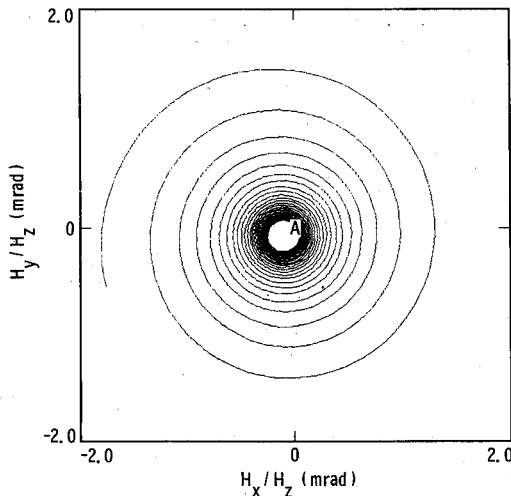


Fig. 9 Nominal orientation of the angular momentum vector in inertial space during spindown maneuver.

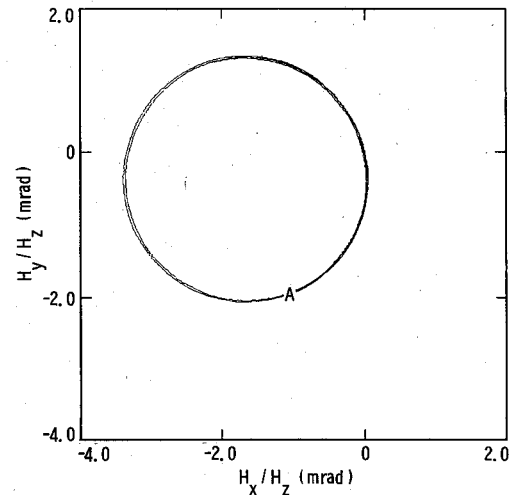


Fig. 11 Variational orientation of  $H_f$  during spindown for  $\omega_{z0} \pm 50\%$ .

Hence, since the parameters are independent, the secular uncertainty about the average may be estimated by the following equation.

$$\sigma_{\rho 0} = (\sigma_M^2 + \sigma_{Iz}^2 + 4\sigma_{\omega z}^2)^{1/2} \quad (9)$$

The simulation results for the periodic errors show that the final momentum vector due to these parameter variations will trace a circle about an average point which is given by Eqs. (6). This result suggests a narrow width ring distribution model for the variations of the periodic effects. To simplify the analysis a zero-width ring distribution, Fig. 14, is assumed, which implies that the probability density function with respect to  $r$  is impulsive.

$$f(r) = \delta(r - R) \quad (10)$$

Furthermore, a uniform distribution in  $\theta$  is assumed, i.e.,

$$f(\theta) = 1/(2\pi), \quad 0 < \theta < 2\pi \\ = 0, \quad \text{otherwise} \quad (11)$$

These assumptions imply that the momentum vector points, with equal probability, to any location on the perimeter of a circle the center of which is given by Eqs. (6) and the radius is

$R$ . In effect, this defines a cone about the average pointing direction, given by Eqs. (5) and (6), the trace of which in the  $x$ - $y$  plane is a circle that may be estimated as follows:

It may be shown that the probability density function in terms of one of the Cartesian coordinates, say  $x$ , will be given by

$$f(x) = (R^2 - x^2)^{-1/2} / \pi, \quad -R < x < R \\ = 0, \quad \text{otherwise} \quad (12)$$

where mean and variance for this distribution are given as 0 and  $R^2/2$ , respectively. The distribution plot is shown in Fig. 15.

In the application to the Galileo spacecraft we are interested in the  $3\sigma$  dispersions of the angular momentum vector, which corresponds to 99.7% level of confidence for a Gaussian distribution. For the ring distribution it is easily shown that the 99.7% level of confidence will occur at  $x=R$ . The heuristic solution, Eq. (5), gives a good estimate of  $R$  for any  $\omega_z(t)$ . The circle of interest is the trace of the momentum vector  $H(t)$  at  $t=t_f$ . Hence Eq. (5) with  $\omega_z = \omega_{zf}$  gives a good approximation to the 99.7% confidence circle of uncertainty.

By combining the above results we obtain a simple probabilistic model for the pointing error, Fig. 16. The final

angular momentum vector will point, with 99.7% probability, within a circle of radius  $R_t$  about the average pointing vector  $\rho_0$ , where

$$R_t = 3\sigma_{\rho_0} + R \quad (13)$$

The numerical values of the parameters used in the simulation and the result of the deterministic performance analysis are summarized in Table 1. Using these parameter

values the estimated ring radius is calculated as 0.146 mrad, in close agreement with the results given in Table 1.

Finally, a Monte Carlo simulation was performed. For the parameters producing periodic effects the Monte Carlo simulation resulted in 1.69 mrad mean and 0.1079 mrad  $1\sigma$  values. These values compare favorably to 1.708 and 0.1032 mrad estimated mean and  $1\sigma$  values.

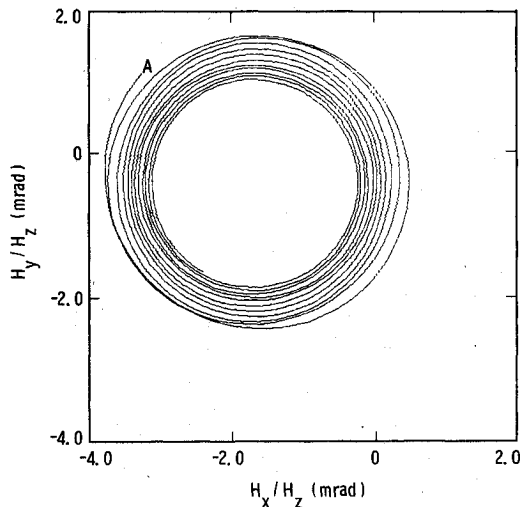


Fig. 12 Variational orientation of  $H_f$  during spindown for  $I_z \pm 20\%$ .

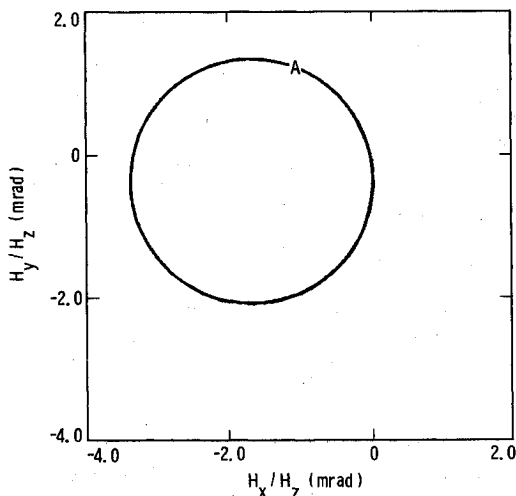


Fig. 13 Variational orientation of  $H_f$  during spindown for  $M_z \pm 50\%$ .

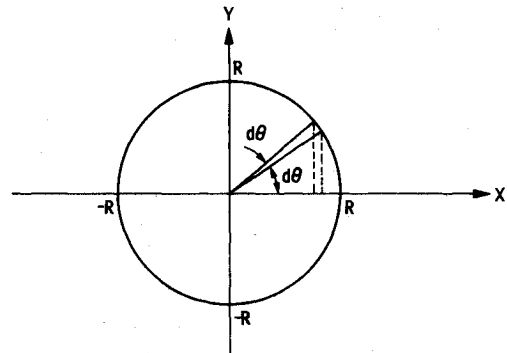


Fig. 14 Zero width ring distribution.

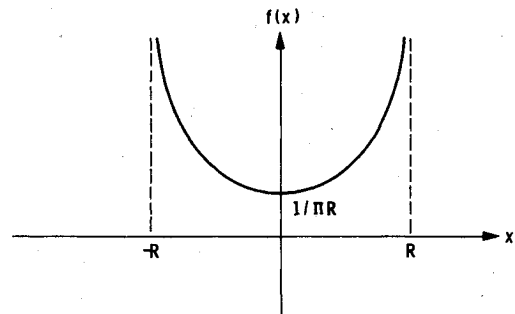


Fig. 15 Zero width ring distribution in Cartesian coordinates.

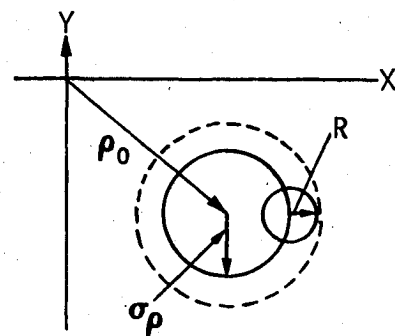


Fig. 16 Pointing error model for the spin-change maneuver.

Table 1 Deterministic performance analysis results

Error source	Nominal source value	Source error, %	Resultant secular error, mrad	Periodic radius of uncertainty, mrad
$I_x$	3012 kg-m <sup>2</sup>	2.1	0.00381	—
$I_y$	2716 kg-m <sup>2</sup>	2.4	0.00479	—
$I_z$	4627 kg-m <sup>2</sup>	1.5	0.04	0.15
$M_x$	-0.4757 N-m	5.1	0.0585	—
$M_y$	-0.5669 N-m	5.1	0.0699	—
$M_z$	13.0 N-m	5.1	—	0.147
$\omega_{z0}$	0.306 rad/s	6.8 <sup>a</sup>	0.225	—
$\omega_{zf}$	1.047 rad/s	17	0.07	0.135
Total error			0.247	0.15

<sup>a</sup> Uniform distribution.

### Conclusions

The form of a highly accurate approximate analytic solution is presented for the angular momentum vector for near-symmetric rigid bodies subject to constant moments. The solution is given as a function of the Eulerian angles and the angular velocities, which were solved for in a previous paper. The solution applies when two of the Eulerian angles are small and a certain parameter is large. This analytic result permits the parametric behavior of the angular momentum vector to be studied during spin rate change maneuvers such as occur in the Galileo mission to Jupiter. For this particular case, simple heuristic formulas were discovered which aid greatly in obtaining quick numerical results. While it would not be wise to extend these heuristic results to the general case, the basic approach can be used to study a variety of interesting cases using the same analytic solution, without which such studies would be prohibitively expensive and time consuming due to the many computer simulations required.

### Acknowledgments

The authors thank W. G. Breckenridge for his helpful suggestions and Pat Warmer for typing the original manuscript.

The research described in this paper was carried out by the Jet Propulsion Laboratory, California Institute of Technology, under contract with the National Aeronautics and Space Administration.

### References

- <sup>1</sup>Longuski, J.M., "Solutions of Euler's Equations of Motion and Eulerian Angles for Near Symmetric Rigid Bodies Subject to Constant Moments," AIAA Paper 80-1642, Danvers, Mass., Aug. 1980.
- <sup>2</sup>Bödewadt, U.T., "Der symmetrische Kreisel bei zeitfester Drehkraft," *Mathematische Zeitschrift*, 55, 1952, pp. 310-320.
- <sup>3</sup>Wertz, J.R., *Spacecraft Attitude Determination and Control*, D. Reidel Publishing Co., Dordrecht, Holland, 1980.
- <sup>4</sup>Longuski, J.M., "Comments on the Leimanis Solution of Self-Excited Rigid Body," Paper 81-104, AAS/AIAA Astrodynamics Conference, Lake Tahoe, Nev., Aug. 1981. Accepted for publication by the *Journal of the Astronautical Sciences*.
- <sup>5</sup>Leimanis, E., *The General Problem of the Motion of Coupled Rigid Bodies About a Fixed Point*, Springer-Verlag, New York, 1965.

*From the AIAA Progress in Astronautics and Aeronautics Series . . .*

## RADIATIVE TRANSFER AND THERMAL CONTROL—v. 49

*Edited by Allie M. Smith, ARO, Inc., Arnold Air Force Station, Tennessee*

This volume is concerned with the mechanisms of heat transfer, a subject that is regarded as classical in the field of engineering. However, as sometimes happens in science and engineering, modern technological challenges arise in the course of events that compel the expansion of even a well-established field far beyond its classical boundaries. This has been the case in the field of heat transfer as problems arose in space flight, in re-entry into Earth's atmosphere, and in entry into such extreme atmospheric environments as that of Venus. Problems of radiative transfer in empty space, conductance and contact resistances among conductors within a spacecraft, gaseous radiation in complex environments, interactions with solar radiation, the physical properties of materials under space conditions, and the novel characteristics of that rather special device, the heat pipe—all of these are the subject of this volume.

The editor has addressed this volume to the large community of heat transfer scientists and engineers who wish to keep abreast of their field as it expands into these new territories.

*569 pp., 6x9, illus., \$19.00 Mem. \$40.00 List*

TO ORDER WRITE: Publications Order Dept., AIAA, 1633 Broadway, New York, N.Y. 10019